Osmotic Water Permeability of Human Red Cells

T. C. TERWILLIGER and A. K. SOLOMON

From the Biophysical Laboratory, Harvard Medical School, Boston, Massachusetts 02115. T. C. Terwilliger's present address is Molecular Biology Institute, University of California, Los Angeles, California 90024.

ABSTRACT The osmotic water permeability of human red cells has been reexamined with a stopped-flow device and a new perturbation technique. Small osmotic gradients are used to minimize the systematic error caused by nonlinearities in the relationship between cell volume and light scattering. Corrections are then made for residual systematic error. Our results show that the hydraulic conductivity, L_p, is essentially independent of the direction of water flow and of osmolality in the range 184–365 mosM. The mean value of L_p obtained was 1.8 ± 0.1 (SEM) $\times 10^{-11}$ cm^3 dyne^{-1} s^{-1}.

INTRODUCTION

The permeability of human red cells to water under an osmotic pressure gradient has been investigated in several laboratories (Sidel and Solomon, 1957; Sha'afi et al., 1967; Rich et al., 1968; Farmer and Macey, 1970; Blum and Forster, 1970; Colombe and Macey, 1974; Galey, 1978; Papanek, 1978; Levin et al., 1980) by methods using the intensity of light scattered by, or transmitted through, a suspension of cells as a measure of cell volume. All these experiments have depended upon the assumption that the scattered light intensity is linearly related to the volume of the cells. However, Levin et al. (1980) have recently shown, in an apparatus similar to ours, that this linear relationship is not an accurate representation of light scattering, at equilibrium. Additionally, when stop-flow devices are used to measure cell volume changes, there is a well-known artifactual change in scattered light intensity that occurs when the flow is stopped. Blum and Forster (1970) found that the magnitude of this mixing artifact depends on the volume of the cells in suspension; the problem has also been treated extensively by Papanek (1978).

The present study shows that neglect of the nonlinearities in the light intensity–cell volume relationship may lead to substantial systematic error in determinations of cell volume and presents a procedure to correct for this error. This method has been used in a set of experiments that employ a perturbation technique to study the effects of both the osmolality of the suspension medium and the direction of water flow on the hydraulic conductivity, L_p. The results show that L_p is essentially independent of both osmolality and flow direction. The observation that osmotic water flow across the red

J. GEN. PHYSIOL. © The Rockefeller University Press · 0022-1295/81/05/0549/22 $1.00 549
Volume 77 May 1981 549–570

cell membrane does not depend on the direction of flow is in agreement with the findings of Rich et al. (1968) but at variance with the conclusions of Farmer and Macey (1970).

THEORY

Perturbation Method

When the red cell volume changes in each experiment are small, as in the present study, a perturbation method may be used to calculate changes in red cell volume from measured changes in the light scattering properties of the cells. Let us assume that the intensity of light scattered in a stop-flow apparatus is a single-valued function of time and cell volume. The intensity of light $I(V,t)$ scattered at a time after mixing, t, by cells of arbitrary volume, V, may then be expressed in terms of the intensity of light $I(V_0,t)$ scattered at the same time after mixing by a control suspension of red cells that have a constant cell volume, V_0,

$$I(V,t) \approx I(V_0,t) + a(V_0,t)(V - V_0) + b(t)(V - V_0)^2/2, \tag{1}$$

where we have included terms only to second order in $(V - V_0)$. In this approximation, the coefficients $a(V_0,t)$ and $b(t)$ are time dependent, but only $a(V_0,t)$, the first derivative of I with respect to V, depends on the volume of the control cells:

$$a(V_0,t) = \left.\frac{\partial I(V,t)}{\partial V}\right|_{V_0}. \tag{1 a}$$

The coefficient $b(t)$ is given by the average value of the second derivative of I with respect to V over the cell volume included in a set of experiments:

$$b(t) = \left\langle \frac{\partial^2 I(V,t)}{\partial V^2} \right\rangle. \tag{1 b}$$

Over this range of cell volumes, then, $a(V,t)$ and $b(t)$ are related by,

$$a(V,t) \approx a(V_1,t) + b(t)(V - V_1) \tag{1 c}$$

for arbitrary volumes, V and V_1.

We now define a difference function $I_{DIF}(V,V_0,t)$ as the difference at time, t, between the intensity of light scattered by cells of volume, V, in the experimental suspension and the intensity of light scattered by control cells of constant volume, V_0:

$$I_{DIF}(V,V_0,t) \equiv I(V,t) - I(V_0,t). \tag{2}$$

Hence,

$$I_{DIF}(V,V_0,t) \approx a(V_0,t)(V - V_0) + b(t)(V - V_0)^2/2 \tag{1'}$$

The difference function is the portion of the intensity of scattered light related to the difference between the volumes of the cells in the two suspensions. For simplicity, a time-independent linear approximation to Eq. 1′ has been used,

followed by partial corrections for the actual time dependence and nonlinearity.

In each of the present experiments two separate constant cell volumes have been used as controls, rather than the one isosmolal cell volume previously used (Rich et al., 1968). The two volumes chosen were the initial volume (V_i) and the final volume (V_f) of the cells in each experiment. When the initial volume was used, the initial approximation to Eq. 1′ was

$$I_{DIF}(V,V_i,t) \approx C(V - V_i), \tag{3}$$

in which the constant, C, was determined from the initial and final cell volumes and intensitites of scattered light (see Appendix). The light scattered by this control suspension $[I(V_i,t)]$ and by a suspension of cells with unknown volume $[I(V,t)]$ was used to approximate the unknown volume, $V(t)$, by the function $V'(t)$, using Eq. 3,

$$V'(t) = V_i + (1/C)I_{DIF}(V,V_i,t). \tag{4}$$

Using Eqs. 1′, 1 *c*, and 4, it can be shown that the difference, $\delta V(t)$, between the true volume, $V(t)$, and the approximation to it, $V'(t)$, is to second order (see Appendix),

$$\delta V(t) \approx \frac{\bar{b}(V - V_i)(V_f - V)}{2a(\bar{V},t_f)} + \frac{[a(\bar{V},t_f) - a(\bar{V},t)](V - V_i)}{a(\bar{V},t_f)}, \tag{5}$$

where t_i is the initial time, t_f is the time at which final cell volumes and intensities of scattered light are calculated, $\bar{b}$ is $[b(t_i) + b(t_f)]/2$, and $\bar{V}$ is at the average volume of the cells during the experiment $[\bar{V} = (V_i + V_f)/2]$. The first term in Eq. 5 is due to the dependence of the derivative, $a(V,t)$, in Eq. 1 *c* on cell volume; the second term is related to the dependence of $a(V,t)$ on time. With minor changes, these calculations may be repeated using cells of the final volume, V_f, in the control suspension, leading to equations similar to Eqs. 3–5.

Calculation of L_p

When a steady state has been established in a system close to equilibrium, in the absence of permeable solute and hydrostatic pressure differences, the theory of Kedem and Katchalsky (1958) gives the following equation for the rate of bulk flow of water, J_v, across a membrane:

$$J_v = RTL_p(\pi_i - \pi_o), \tag{6}$$

in which L_p is the hydraulic conductivity of the membrane, π_i and π_o are the osmolalities of the solutions on the two sides of the membrane, and R and T have their usual meanings. We have assumed that the Kedem and Katchalsky conditions are fulfilled (see Appendix), that a constant extracellular osmolality has been established immediately after mixing, that intracellular mixing is instantaneous (see Paganelli and Solomon [1957] and Papanek [1978]), and that temperature does not change during an experiment. Assuming that the osmotic coefficients of the intracellular solutes do not change over the concen-

tration range in these experiments, and that apparent nonosmotic volume is constant, we can write

$$V = V_b + \frac{\pi_{iso}}{\pi}(V_{iso} - V_b), \tag{7}$$

where V, V_{iso}, π, and π_{iso} are the cell volumes and intracellular osmolalities under experimental and isosmolal conditions, respectively, and where V_b is the apparent nonosmotic volume (Savitz et al., 1964). L_p and other membrane parameters, including the effective membrane area, are assumed to remain constant during the course of an experiment.

With these assumptions, Eq. 6 can be integrated using Eq. 7 to obtain

$$L_p = \frac{(V_{iso} - V_b)\,\pi_{iso}}{tART(\pi_f)^2}\left\{S(t)\left(\frac{\pi_f}{\pi_i} - 1\right) - \ln\left[1 - S(t)\right]\right\}, \tag{8}$$

in which A and V_{iso} are the isosmotic red cell surface area and volume, taken to be 137 μm^2 and 104 μm^3, after Jay (1975); π_{iso}, π_i, and π_f are the osmolalities of an isosmolar solution (290 mosM), the extracellular solution before mixing, and the extracellular solution after mixing; t is the time after effective mixing of the two solutions and $S(t)$ is the fraction of the final cell volume change that has occurred by time t. Using Eq. 4, $S(t)$ can be determined using experimentally measurable quantities

$$S(t) \equiv \frac{V(t) - V_i}{V_f - V_i} \approx \frac{I_{DIF}(V,V_0,t) - I_{DIF}(V_i,V_0,t_i)}{I_{DIF}(V_f,V_0,t_f) - I_{DIF}(V_i,V_0,t_i)}, \tag{9}$$

in which $I_{DIF}(V,V_0,t)$ is a difference function for the experiment obtained using cells of volume, V_0, equal to V_i or V_f, in the control runs, t_i is the initial time, and t_f is the time at which final cell volume and osmolalities are calculated.

The value of L_p for each combination of experimental and control runs was calculated using a three-parameter fitting routine. This routine found the values of L_p, $I_{DIF}(V_i,V_0,t_i)$, and $I_{DIF}(V_f,V_0,t_f)$ that minimized the reduced χ^2,

$$\chi^2_v = \frac{1}{n-3}\sum_{j=1}^{n}\frac{(L_p(t_j) - \bar{L}_p)^2}{\sigma_j^2}, \tag{10}$$

where $\bar{L}_p$ is the average value of L_p calculated for the experiment, using Eqs. 8 and 9,

$$\bar{L}_p = \frac{\sum_{j=1}^{n} L_p\,(t_j)/\sigma_j^2}{\sum_{j=1}^{n} 1/\sigma_j^2}. \tag{11}$$

The subscript j refers to a calculation of L_p at time, t_j, and the weighting factors σ_j^2 are discussed in the Appendix. For each calculation of $\bar{L}_p$ and χ^2_v, all the data obtained between the time of mixing and a time, t, at which $S(t)$ was at least equal to 0.92 were used in the fitting program.

As shown by Eq. 5, inaccurate determinations of cell volume may result if it is assumed that a linear relationship exists between changes in V and changes in $I_{DIF}(V,V_0,t)$. To correct for these errors in $\bar{L}_p$, we note that the error, $\delta L_p(t_j)$, in the value of L_p calculated at time, t_j, is roughly given by

$$\delta L_p(t_j) = -\frac{\partial L_p}{\partial V}\delta V(t_j), \tag{12}$$

where $\delta V(t_j)$ is the difference between the true cell volume and the cell volume at time, t_j, given approximately in Eq. 5. For the case in which the difference function was obtained using control cells equal in volume to that of the experimental cells at zero time, equations 5, 8, 9, and 12 lead to an error in a calculation (see Appendix) of L_p at time, t_j, of

$$\frac{\delta L_p(t_j)}{\bar{L}_p} \approx \frac{\Delta V\bar{b}}{2\,a(\bar{V},t_f)}\frac{S(t_j)}{\ln[1-S(t_j)]} + \frac{a(\bar{V},t_f)-a(\bar{V},t_i)}{a(\bar{V},t_f)}\frac{S(t_j)[1-T(t_j)]}{[1-S(t_j)]\ln[1-S(t_j)]}. \tag{13}$$

Eq. 13 is applicable when ΔV, the total volume change of the red cells during the experiment is small. The function, $T(t)$, is the fractional change in the derivative $a(\bar{V},t)$ in Eq. 1 that has occurred by time t,

$$T(t) \equiv \frac{a(\bar{V},t)-a(\bar{V},t_i)}{a(\bar{V},t_f)-a(\bar{V},t_i)}, \tag{14}$$

where t_i and t_f are as previously defined. The correction applied to the average value of L_p for a combination of experimental and control runs was

$$\frac{\delta\bar{L}_p}{\bar{L}_p} \approx -\frac{\Delta V\bar{b}}{2\,a(\bar{V},t_f)}F_1 - \frac{a(\bar{V},t_f)-a(\bar{V},t_i)}{a(\bar{V},t_f)}F_2, \tag{15}$$

where F_1 and F_2 are the weighted averages of the functions $S(t)/\ln[1-S(t)]$ and $S(t)[1-T(t)]/\{[1-S(t)]\ln[1-S(t)]\}$ for the experiment.

Repeating these calculations for the case in which cells of the final equilibrium volume in the experimental runs were used as controls, the correction in $\bar{L}_p$ was given by,

$$\frac{\delta\bar{L}_p}{\bar{L}_p} = -\frac{\Delta V\bar{b}}{2a(\bar{V},t_i)}F_1 - \frac{a(\bar{V},t_f)-a(\bar{V},t_i)}{a(\bar{V},t_i)}F_3, \tag{16}$$

where F_3 is the weighted average of the function $T(t)/\ln[1-S(t)]$ for the experiment. To simplify our calculations, we have assumed that the weighting factors and the functions $S(t)$ and $T(t)$ have the same time dependence for all experiments, and hence that F_1, F_2, and F_3 are constants (see Appendix). The reported value of L_p for a given experimental run is the average of the values obtained and corrected in this manner, using the two control sets of data for the experiment.

APPARATUS AND METHODS

Stop-Flow Apparatus

The stop-flow apparatus described by Levin et al. (1980) has been redesigned and rebuilt. The electronic circuitry, the mixing chamber, and the observation tube are unaltered, but the stopping mechanism and the optical system have been changed. In the previous apparatus, the mixture of red cells and buffer solution was forced through an observation tube and into a collecting syringe, where it drove a piston toward a rubber-padded stop block. When the piston struck the block, flow was halted. During the next 2–5 s, a photodiode detected the intensity of 90° scattered white light from the suspension in the observation tube. Throughout the cycle, the drive syringes maintained an internal pressure of 50 atm on the fluid system. In the current device shown in Fig. 1, the solutions are driven in the same manner, but the drive unit is stopped, rather than the piston of the collecting syringe. Hence, the fluid pressure is lowered upon stopping; a pressure of ~5 atm is applied to the fluid in the collecting syringe to prevent cavitation of the fluid during deceleration.

The observation tube in the previous apparatus was illuminated with a nonfocusing light pipe. To minimize extraneous scattering off the edge of the observation tube, the light pipe has now been replaced by a set of lenses. At the observation tube, which has a width of ~2.2 mm, the beam is focused into an area ~1.0 mm wide and 2.5 mm high.

Experimental Procedure

In each of four sets of experiments, 100–150 ml of blood were drawn by venipuncture from a healthy human donor and placed in a heparinized flask (1,000 USP U/100 ml blood). The blood was immediately centrifuged and the supernatant fluid and buffy coat were removed by aspiration. The cells were then washed twice in a 296 ± 2 mosM buffer solution. The final packed cell suspension contained ~13% buffer by volume. This was diluted to 45–65% buffer to facilitate pipetting. 5- or 10-ml aliquots of this suspension were pipetted into each of a set of beakers containing 200 ml of buffer solutions of various osmolalities. The buffers contained (mM): NaCl, 12.5–400; KCl, 4.4; $NaHCO_3$, 24.9; $CaCl_2$, 1.2; $MgCl_2$, 0.5; Na_2HPO_4, 5.9. The pH of the solutions were adjusted to pH 7.2–7.4 by passing a mixture of 5% CO_2–95% air through them. Osmolalities of the solutions were measured using a Fiske model OS osmometer (Fiske Associates Inc., Uxbridge, Mass.). All solutions and cell suspensions were kept in water baths, and the temperature of each cell suspension was monitored before and after use. Corrections for apparent nonosmotic volume were made according to the procedure of Savitz et al. (1964), and stop-flow dead time was measured by the procedure of Papanek (1978).

For experimental runs, the red cell suspensions were mixed with buffer differing in osmolality from the cell suspension by 40–100 mosM. After the flow stopped, the scattered light intensity was sampled at 4.5- to 5.0-ms intervals over a period of 4.5–5.0 s as described by Levin et al. (1980). This process was repeated 10 to 30 times for each pair of solutions; the experimental set of data consisted of the average of the values obtained at each sampling time. The order of osmolality of the runs was randomized as a standard part of the experimental design.

The control sets of data were obtained in the same manner, except that the cell suspensions were mixed with solutions within 3 mosM of the cell suspension osmolality. One control set of data was obtained with cells of the initial volume and the other was obtained with cells of the final equilibrium volume in each experimental run. The determination of the values of the derivatives $a(V,t_i)$, $a(V,t_f)$, and $\bar{b}$ in Eq. 15 and 16 and of the constants, F_1, F_2, F_3 is discussed in the Appendix.

To measure the effect of the index of refraction on light scattered in the presence and absence of red cells we prepared two sets of solutions of various osmolalities, one varying primarily in the concentration of NaCl, the other varying primarily in the concentration of sucrose. The concentrations in the first set varied from 65 mM NaCl and 2 mM sucrose to 190 mM NaCl and 20 mM sucrose. The second set contained 50 mM NaCl and sucrose in concentrations varying from 24 to 240 mM. A buffer solution containing 90 mM NaCl with, or without, red cells was mixed in the apparatus with each of these solutions in turn, and light intensity was measured. All the solutions in this experiment contained the standard buffer constituents given above.

Table I summarizes the experimental conditions for each set of experiments. The

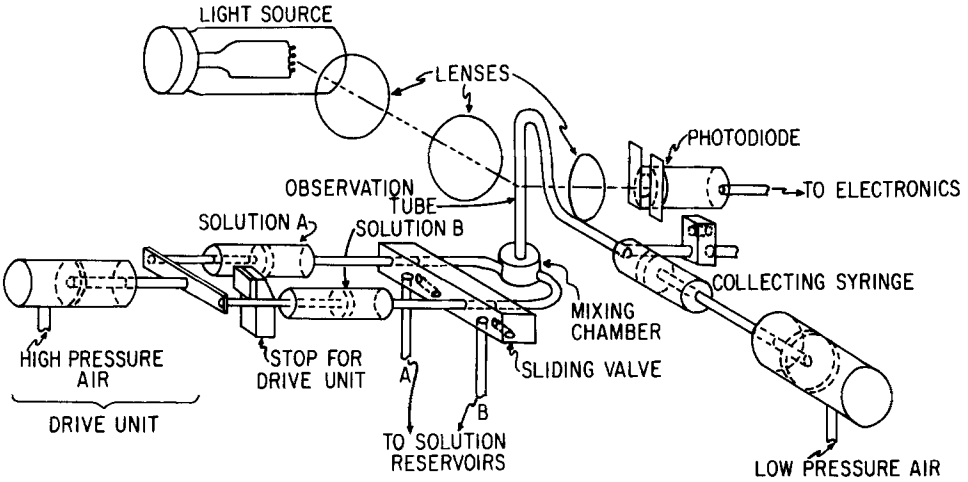

FIGURE 1. Schematic representation of stop-flow apparatus. When high pressure air is forced into drive unit, solutions A and B are driven from syringes into the mixing chamber, through the observation tube, and into the collecting syringe. Flow is halted when the drive unit strikes the stop block. After the flow is stopped, the intensity of 90° scattered light is monitored with a photodiode detector. Low-pressure air is used to apply a constant pressure to the fluid in the collecting syringe throughout the cycle.

conditions were quite similar in the four sets of experiments, except for pH, which was normally measured at the beginning of each run and at its close, some 3 h later. The figures in Table I are the average of these values. The excursions were limited to the range of 7.2 to 7.9, except those for donor 3, which changed from pH 7.4 before the run to pH 8.3 afterward. We do not consider these differences in the mean pH among the four experiments to be significant, since Rich et al. (1968) have shown that L_p is independent of pH over the entire range they studied, pH 6–8. They also found that the value of L_p in a bicarbonate buffer similar to the one we have used, which was chosen to simulate human plasma, does not differ from the value of L_p obtained when phosphate was substituted for bicarbonate.

The possibility exists that a pH gradient might have been present between the two solutions that were brought together in the mixing chamber in individual trials. If the same gradient was present in the controls and in the experimental suspension, subtraction of the controls would compensate for any pH gradient-induced volume

changes. However, if there were pH gradients between the cell suspension and its swelling (or shrinking) buffer that were absent in the controls, it would be possible for these gradients to affect the value of L_p. A set of experiments were therefore carried out in which a buffer (shrinking) of pH 7.4 was mixed with cell suspensions of pH 7.4, 7.6, and 7.8. For these experiments, we used a single control buffer (initial cell volume) at pH 7.4. The ratios of L_p at the altered pH to that at pH 7.4 were (in triplicate determinations) 0.95 ± 0.12 and 1.14 ± 0.17 for pH 7.6 and 7.8, respectively. There was no difference in the ratio at pH 7.6 when a control at pH 7.6 was used rather than the pH 7.4 control. When a pH 7.8 control was used at pH 7.8, the ratio became 1.03 ± 0.16. Since none of these ratios is significantly different from 1.0 and since there is no trend, the effect of possible error from pH gradients present during the mixing process has been neglected and is, in any case, subsumed in the errors given in the text.

TABLE I
EXPERIMENTAL CONDITIONS

Donor	Sex	Temperature	pH	Fraction of apparent nonosmotic volume	Flow rate in observation tube	Dead time
		°C		V_b/V_{iso}	$cm\ s^{-1}$	ms
1	M	25±1*	7.5±0.1	0.43±0.01	587±29	14.7±0.4
2	M	26±1	7.5±0.2	0.48±0.02	601±14	14.5±0.2
3	M	26±1	7.9±0.5	0.48±0.02	372±43	17.6±0.6
4	F	25±2	7.4±0.1	0.40±0.02	358±72	17.8±1.0

* Errors are SEM except for temperature and pH, which are SD.

RESULTS AND DISCUSSION

Control Experiments

Light scattered[1] by control red cell suspensions depended strongly on both the volume of the cells and on time, as Fig. 2 shows. The fluctuations with time were much greater when the cells were shrunk in solutions of high osmolality than when they were swollen in solutions of low osmolality. Consequently, the osmolalities used in these experiments were limited to the range of 184–365 mosM, in which the scattering always had the general form shown in the top two curves in Fig 2. Even in this range, however, the difference between the intensities of light scattered by two control suspensions was not constant. Consequently, the derivative $a(V_0,t)$ in Eq. 1 was a function of time. In addition to this time dependence, the intensity of scattered light depended nonlinearly on the red cell volume, in agreement with the observations of Levin et al. (1980). Fig. 3 shows this relationship.

Effect of the Index of Refraction

Fig 4. shows the dependence of light scattering on the index of refraction of NaCl and sucrose solutions. In the absence of cells (*top*), changes in the index

[1] For clarity in presentation, we have followed the convention (Levin et al., 1980) that the change in light scattering due to an increase in cell volume will be represented by an increase in computer units. In fact, the scattered light intensity decreases in this case.

of refraction (Δn) of the solutions caused only small changes in the intensity of scattered light. The effect of the index of refraction on light scattering from red cell suspensions after correction for the scattering of the buffer alone is shown in the lower part of Fig. 4. Eq. 17 gives the approximate relation between changes in scattered light due to changes both in cell volume and in the index of refraction.

$$\Delta I \approx (1.1 \pm 0.1)\ (\Delta V/V_{iso}) + (25 \pm 4)\ \Delta n. \quad (17)$$

Thus, a change in external index of refraction of 0.0004 (equivalent to 40 mM NaCl) causes a change in the intensity of scattered light equal to that

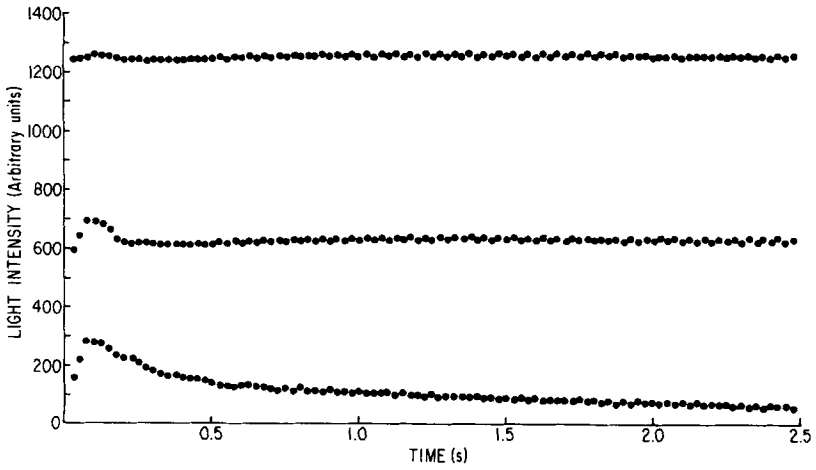

FIGURE 2. Light scattered in control experiments. Each curve is the smoothed average of ten to fifteen runs under identical conditions using red cells from donor 4. The osmolalities and relative cell volumes were 185 mosM (*top*; $V/V_{iso} = 1.34$), 296 mosM (*center*; $V/V_{iso} = 0.99$); and 408 mosM (*bottom*; $V/V_{iso} = 0.83$). Computer units are arbitrary numbers linearly related to the negative of light scattering intensity.

caused by a 1% cell volume change. In the present experiments, dilute solutions of cells have been used and no permeable solutes were present, so the intracellular composition is a function of cell volume only and the external index of refraction is essentially time independent. Consequently the dependence of light scattering on the index of refraction of the medium does not cause significant error in our determinations of cell volume. The results are, nevertheless, presented as a guide for other experiments in which the effect may be appreciable.

Determination of L_p

The curve labeled *Experiment* in Fig. 5 shows the data for a typical experiment in which the cells swell from an initial normalized volume of 0.987 to a final volume of 1.034. The initial control curve in Fig. 5 shows the intensity of light

scattered by cells with a constant volume of 0.987; the final control is that scattered by cells with an essentially constant volume[2] of 1.037. At zero time, the scattering in the experimental run is about the same as for the initial control. During the next second, the light scattered by the experimental suspension changes to roughly that of the final control. After ~1.5 s, the differences among the light scattered by the three suspensions remain fairly constant.

These experiments have been designed to minimize experimental error, and we have therefore exposed the cells to the smallest possible osmotic gradient. This precaution minimizes the effect of nonlinearities in the relationship

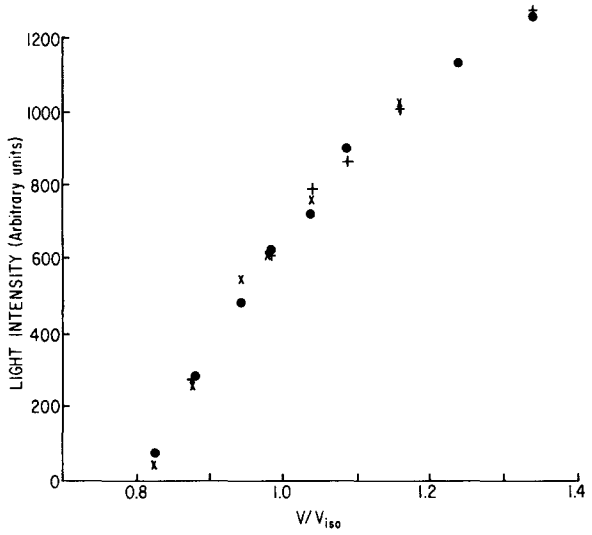

FIGURE 3. Dependence of light scattering intensity on red cell volume. The intensity of light at 2.0 s after mixing by red cells that had swelled (+), shrunk (×), or remained at constant volume (●) are shown as a function of normalized cell volume in one experiment (donor 4), typical of all.

between cell volume and the light scattering intensity by reducing the magnitude of the first term in Eq. 13. This term had the effect of systematically increasing the observed difference in L_p between influx and outflux, because its sign was different in the two cases. Nonetheless, this procedure did not completely eliminate the need for corrections, since the second term in Eq. 13 is relatively independent of the volume change. The effect of this term (before corrections using Eqs. 15 and 16) was primarily to increase the apparent dependence of L_p on osmolality (see Appendix).

Fig. 6 shows the differences between the experimental curve and each of the two control curves shown in Fig. 5. At this stage, it was assumed that the values of the differences were linearly related to the volume of the red cells.

[2] The volume of these red cells increased by ~0.2% over the time period shown.

Using the χ^2 minimization technique given in Eq. 10, the difference curves were analyzed over the time period when the function appeared to be exponential. For the data in Fig. 6, this time began with the first data point (at ~0.02 s after mixing) and ran to 1.26 s (initial control) and 1.70 s (final

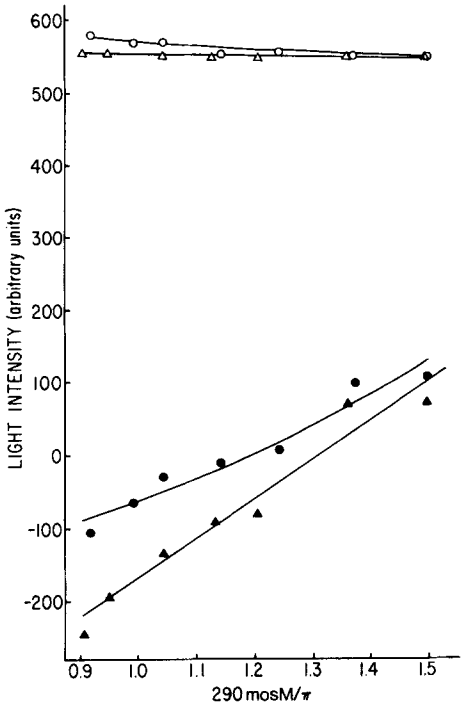

FIGURE 4. Dependence of the intensity of scattered light on the index of refraction. (*Top*) Cell-free solutions of NaCl (triangles) and sucrose (circles). Changes in the index of refraction in the sucrose solution are given by $\Delta n \approx 4.3 \times 10^{-5} \Delta\pi$. Changes in the index of refraction in the NaCl solution are given by $\Delta n \approx 0.94 \times 10^{-5} \Delta\pi$. Both curves drawn are given by $I \approx 547 + 4{,}400\ \delta n$, where δn is the calculated index of refraction relative to a reference solution (with $n = 1.330$). (*Bottom*) Red cell suspensions. The solutions used were identical to those used to obtain the data in the upper figure. The curves drawn are for the least squares regression line $I = -1{,}292 + 29{,}400\ \delta n + 1{,}080\ V/V_{iso}$. Cell volume was assumed to be related to osmolality by the relation $V/V_{iso} = 0.42 + 0.58\ (290/\pi)$.

control). In Fig. 7, the difference functions in Fig. 6 have been converted to normalized volume units, using Eq. 9.

Eqs. 15 and 16 were used to correct these values of L_p for errors incurred by neglecting the nonlinearities and time dependence in Eq. 1′. This procedure led to corrections of +16% to $L_p = 2.4 \pm 0.5 \times 10^{-11}$ cm^3 dyne^{-1} s^{-1} using the initial control and of +4% to $L_p = 1.9 \pm 0.3 \times 10^{-11}$ cm^3 dyne^{-1} s^{-1} using the

final control. They were averaged to obtain a final value of $L_p = 2.0 \pm 0.4 \times 10^{-11}$ cm^3 dyne^{-1} s^{-1} for this swelling experiment. The corrections applied to the calculated values of L_p in the four sets of experiments varied from −30% to +30%, with a weighted average of −4% for swelling experiments and +10% for shrinking experiments. Table II shows the individual L_p values obtained with donor 4, together with the relevant correction factors, and Fig. 8 gives the values of L_p found in each set of experiments multiplied by scaling factors[3] and plotted as a function of inverse extracellular osmolality.

To determine whether there were biological differences among the red cells of the four donors, we calculated the average values of L_p at $\pi_{iso}/\pi = 1$ and

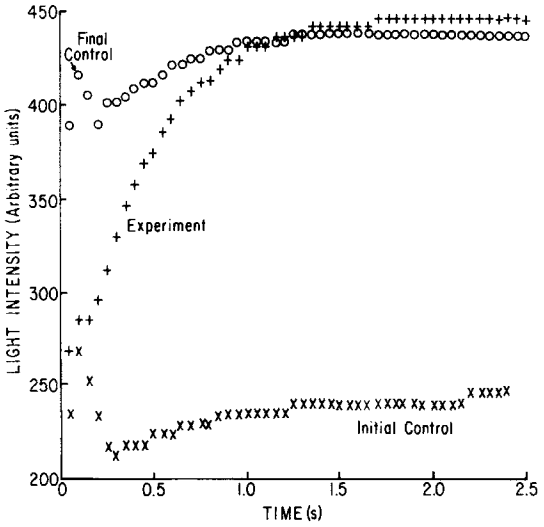

FIGURE 5. Comparison of experimental data with controls. Each point represents the average value for 20–29 runs under identical conditions using red cells from donor 1 (see text). Every tenth point is plotted.

the associated SEMs for each donor from column 3 of Table III. A χ^2 test, used to examine the agreement of these data with the weighted average, gave a probability <0.001, from which we concluded that biological variations could not be neglected. Therefore, the variation in L_p among individuals was estimated from Table III and was found to be $\approx 0.3 \times 10^{-11}$ cm^3 dyne^{-1} s^{-1}. Including all the uncertainties discussed above, we arrived at a value for L_p of 1.8 ± 0.1 (SEM) $\times 10^{-11}$ cm^3 dyne^{-1} s^{-1} at $\pi_{iso}/\pi = 1.0$, in agreement with the previous determination in this laboratory by Rich et al. (1968) of 1.8×10^{-11}

[3] The scaling factors were determined by minimizing the function $q(\bar{a})$, given by

$$q(\bar{a}) = \sum_k \sum_{i<j} \frac{(a_j L_{p_{kj}} - a_i L_{p_{ki}})^2}{\sigma_{kj}^2 + \sigma_{ki}^2}$$

where a_j is the scaling factor for donor j, $L_{p_{kj}}$ and σ_{kj}^2 are the values of L_p and its variance for the kth combination of initial and final osmolalities of the cell suspension for the jth subject.

cm^3 $dyne^{-1}$ s^{-1} (after conversion to the present values for red cell area and volume). The present value is slightly larger than that of $1.3 \pm 0.3 \times 10^{-11}$ cm^3 $dyne^{-1}$ s^{-1} obtained by Papanek (1978) at $\pi_{iso}/\pi = 0.67$ and agrees with that of $1.84 \pm 0.05 \times 10^{-11}$ cm^3 $dyne^{-1}$ s^{-1} (after conversion) given by Galey (1978).

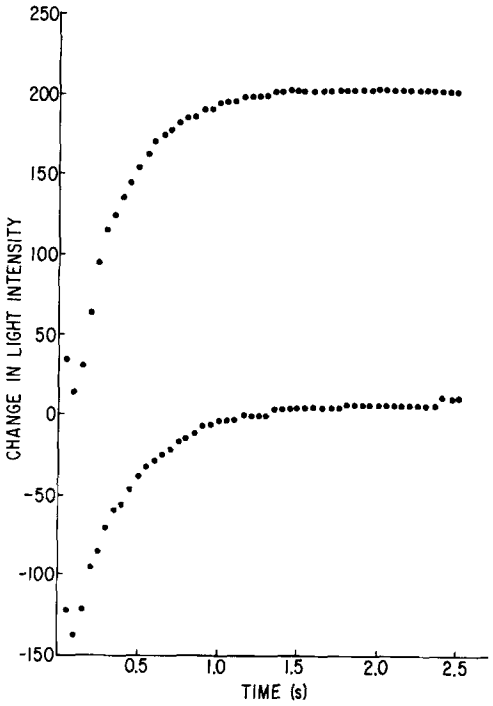

FIGURE 6. Smoothed difference curves for the data in Fig. 5. The *top curve* gives the difference using the initial cell volume in the control runs; the value of the difference function at zero time was calculated to be −44; at equilibrium it was 203. The *bottom curve* uses the control runs at final cell volume; this difference function had a calculated value of −181 at zero time and +5 at equilibrium. Note that the changes in the two different functions between zero time and equilibrium were not equal. This was partially due to the dependence of the derivative $a(\bar{V},t)$ in Eq. 1 on time (see Appendix).

Does L_p Depend on External Osmolality?

The linear regression line in Fig. 8 shows essentially no dependence[4] of L_p on π_{iso}/π; the slope is $-0.1 \pm 0.4 \times 10^{-11}$ cm^3 $dyne^{-1}$ s^{-1}. Previous investigations have found a small dependence of L_p on osmolality. Thus, we can compute from the data of Rich et al. (1968, Fig. 2) that their average L_p is increased by ~37% between $\pi_{iso}/\pi = 0.7$ and 1.0. The Blum and Forster (1970) regression

[4] In these experiments, the cell volume and osmolality are related through Eq. 7. Consequently, it is conceivable, though unlikely, that L_p depends on both in such a fashion that their effects cancel when they are varied together according to Eq. 7.

line increases by 16% over the same range. Neither of these values differs significantly from our result. Column 4 of Table III shows that there may be a difference in the slopes of regression lines for shrinking ($0.7 \pm 0.5 \times 10^{-11}$ cm^3 $dyne^{-1}$ s^{-1}) and swelling ($-0.7 \pm 0.5 \times 10^{-11}$ cm^3 $dyne^{-1}$ s^{-1}) experiments. The errors in the stop-flow method are such that this difference is only marginally significant. As has already been discussed, large osmotic gradients, as previously used, tend to introduce errors that exaggerate the dependence of

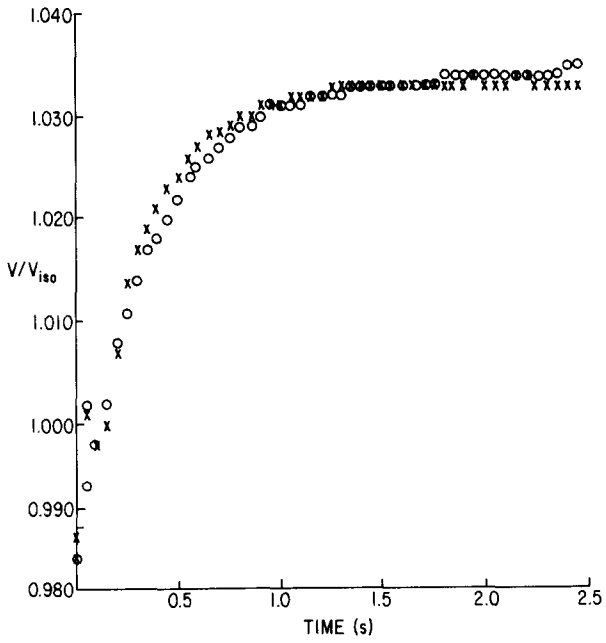

FIGURE 7. Difference functions in volume units. The value of L_p determined from the upper difference function in Fig. 6 before corrections was $2.1 \pm 0.1 \times 10^{-11}$ cm^3 $dyne^{-1}$ s^{-1}. The lower difference function yielded an uncorrected value of L_p of $1.8 \pm 0.1 \times 10^{-11}$ cm^3 $dyne^{-1}$ s^{-1}. (×) Initial control. (○) Final control.

L_p on osmolality. The small osmotic perturbations used in the present experiments and the correction procedures we have applied tend to minimize such errors and to support our conclusion that L_p is independent of external osmolality.

Is There Rectification of Hydraulic Flow?

Though Rich et al. (1968) concluded that there was no rectification of flow, this conclusion has been questioned by Farmer and Macey (1970) and by Blum and Forster (1970). Farmer and Macey found a rectification ratio of 1.39 ± 0.04 ($L_{p,in}/L_{p,out}$), and Blum and Forster a ratio of 1.2. The present experiments were designed to examine this point specifically, and the data in

Fig. 8 show no rectification. When all the experiments in Fig. 8 are taken together, the rectification ratio is 0.95 ± 0.05 (SEM) as shown in the last column in Table III. To examine the effect of any differences in slope of the regression lines between shrinking and swelling expressions, the $L_{p,in}/L_{p,out}$ ratio has been determined at $\pi_{iso}/\pi = 1.0$ for each donor. These data yield a rectification ratio of 1.15 ± 0.10 (reduced $\chi^2 = 1.5$; $P > 0.2$). Though these ratios do not differ significantly from the 1.2 ratio given by Blum and Forster,

TABLE II

DETERMINATION OF L_p IN TYPICAL EXPERIMENT*

$\frac{\bar{V}}{V_{iso}}$	$\frac{\Delta V}{V_{iso}}$	$\frac{\pi_{iso}}{\pi_{final}}$	L_p
	%		$\times 10^{11}$ cm^3 dyne^{-1} s^{-1}
0.91	6.7	0.91	2.19±0.42
0.91	−6.7	0.80	2.21±0.41
0.96	4.1	0.98	2.23±0.39
0.97	−4.0	0.91	1.97±0.34
1.01	−4.8	0.97	1.59±0.25
1.01	4.9	1.06	2.65±0.44
1.06	6.0	1.15	2.78±0.40
1.06	−5.7	1.06	1.80±0.23
1.13	7.0	1.27	2.19±0.23
1.13	−7.0	1.15	2.17±0.22
1.20	−8.1	1.27	2.00±0.15
1.20	8.3	1.41	2.02±0.16
1.29	10.8	1.58	1.76±0.30
1.29	−9.8	1.40	2.06±0.29

Correction factors at $\bar{V} = V_{iso}$‡

$a(t_i)$	$a(t_f)$	$b(t_i)$	$b(t_f)$
2459±200	2976±206	−3824±350	−6331±474

* Data for one experiment with donor 4. Experiments with donors 1-3 gave similar results, except that they were limited to 7-8 osmolalities per donor.

‡ The value for the F constants were the same for all four donors: $F_1 = -0.541 \pm 0.009$; $F_2 = -0.941 \pm 1.156$; $F_3 = -0.316 \pm 0.562$.

they are entirely at variance with the value of 1.39 ± 0.04 reported by Farmer and Macey. In a recent study of the rectification factor, Galey (1978) shrank his red cells by 20% and swelled them by 25% to obtain a rectification ratio of 1.5. This apparent rectification may reflect the result of applying Kedem-Katchalsky equations to uncorrected data taken when the gradients are large. The data presented in the present paper, which were obtained when the gradients were small and to which suitable corrections were applied, show that there is no evidence for rectification of water flow across the human red cell membrane, in agreement with the conclusion reached by Rich et al. (1968).

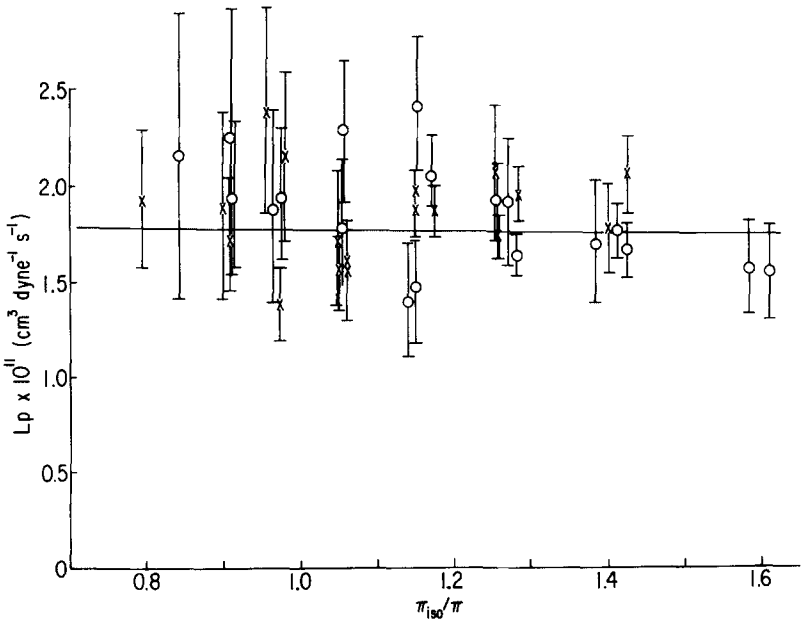

FIGURE 8. L_p as a function of inverse osmolality. Corrected values of L_p for swelling (○) and shrinking (×) experiments have been multiplied by scaling factors for each experiment and plotted as a function of final (π_{iso}/π). The scaling factors used were: donor 1, 0.9 ± 0.1; donor 2, 1.0 ± 0.2; donor 3, 1.23 ± 0.02; donor 4, 0.87 ± 0.04. The error bars shown are SD and include error estimates in the scaling factors. The line drawn is a weighted least squares fit.

TABLE III
DEPENDENCE OF L_p ON DIRECTION OF FLOW

Donor	Flow direction	L_p at $\pi_{iso}/\pi = 1$	Slope, $\Delta L_p/\Delta(\pi_{iso}/\pi)$	$L_{p,in}/L_{p,out}$ (π_{iso}/π) = 1	$L_{p,in}/L_{p,out}$ All experiments
		× 10^{11} cm^3 $dyne^{-1}$ s^{-1}	× 10^{11} cm^3 $dyne^{-1}$ s^{-1}		
1	shrink	2.0±0.3*	1.4±1.6	0.9±0.2	0.9±0.1
	swell	1.9±0.3	0.5±1.3		
2	shrink	1.9±0.1	−2.2±2.5	1.0±0.2	0.8±0.1
	swell	1.8±0.2	−3.0±1.8		
3	shrink	1.2±0.1	1.3±0.5	1.4±0.2	1.0±0.1
	swell	1.7±0.2	−0.8±0.4		
4	shrink	1.9±0.2	0.4±0.7	1.3±0.2	1.1±0.1
	swell	2.4±0.3	−1.0±0.7		
avg‡	shrink	1.7±0.2	0.7±0.5		
	swell	1.9±0.2	−0.7±0.5		
	all	1.8±0.1	−0.1±0.4	1.15±0.10	0.95±0.05

* These error estimates take into account the systematic nature of our uncertainties.
‡ The weighted average for L_p includes the calculated variation between individuals in each weighting factor. The error-weighted averages for the slope consider all the swelling, or shrinking, data together after multiplication by the scaling factors given in the legend to Fig 8.

APPENDIX

Derivation of Eq. 5

Using Eq. 4, the difference $\delta V(t)$ between the true volume, $V(t)$, and the approximation to it, $V'(t)$, is

$$V(t) \equiv V - [V_i + (1/C)I_{DIF}(V,V_i,t)]. \tag{5 a}$$

The constant, C, determined from the initial and final cell volumes and intensities of scattered light, is given by

$$C = [I_{DIF}(V_f,V_i^0,t_f) - I_{DIF}(V_i,V_i^0,t_i)]/(V_f - V_i), \tag{3 a}$$

where the superscript in $I_{DIF}(V_i,V_i^0,t_i)$ is used to emphasize that this difference function is the difference, at time t_i and volume $V_i = V_i^0$, between the scattering from cells that have just been exposed to an osmotic gradient and the scattering from cells in an isosmolal buffer. This term will in general be equal to zero within experimental error. Using Eq. 1′, which is accurate to second order in $(V_f - V_i)$,

$$C \approx a(V_i,t_f) + b(t_f)(V_f - V_i)/2 \tag{3 b}$$

Using Eq. 1 *c*, this becomes

$$C \approx a(\bar{V},t_f), \tag{3 c}$$

where $\bar{V}$ is the average volume of the cells during the experiment, $[\bar{V} = (V_i + V_f)/2]$. Combining this with Eqs. 1′ and 5 *a*, we obtain,

$$\delta V(t) \approx [a(\bar{V},t_f)(V - V_i) - a(V_i,t)(V - V_i) + b(t)(V - V_i)^2/2]/a(\bar{V},t_f). \tag{5 b}$$

Then, using Eq. 1 *c*,

$$\delta V(t) \approx \frac{[a(\bar{V},t_f) - a(\bar{V},t)](V - V_i)}{a(\bar{V},t_f)} + \frac{b(t)(V - V_i)(V_f - V)}{2a(\bar{V},t_f)} \tag{5 c}$$

Finally, dropping the third order term, $[b(t) - \bar{b}](V - V_i)(V_f - V)/[2a(\bar{V},t_f)]$, where $\bar{b}$ is given by

$$\bar{b} = [b(t_i) + b(t_f)]/2, \tag{5 d}$$

we obtain Eq. 5.

Derivation of Eq. 13

For the case in which the difference function was obtained with control cells equal in volume to those in the experimental runs at zero time, t_i, Eqs. 8 and 12 lead to a relative error in a calculation of L_p at time, t_j, of,

$$\frac{\delta L_p(t_j)}{L_p(t_j)} \approx \frac{\left(\left[\frac{\pi_f}{\pi_i} - 1\right] + \left[\frac{1}{1 - S(t_j)}\right]\right)\frac{\partial S(t)}{\partial V}\delta V(t_j)}{\left(\left[\frac{\pi_f}{\pi_i} - 1\right] - \frac{\ln[1 - S(t_j)]}{S(t_j)}\right)S(t_j)} \tag{13 a}$$

If the fractional osmolality change during the experiment, $\pi_f/\pi_i - 1$, is much less than unity, it may be neglected in Eq. 13 *a* to yield,

$$\frac{\delta L_p(t_j)}{L_p(t_j)} \approx \frac{-\frac{\partial S(t)}{\partial V}\delta V(t_j)}{[1 - S(t_j)]\ln[1 - S(t_j)]}. \tag{13 b}$$

Substituting Eqs. 5 and 9, and noting that L_p is essentially constant during an experiment, $L_p(t_j) \approx \bar{L}_p$, we arrive at Eq. 13.

Determination of the Derivatives $a(V,t_i)$, $a(V,t_f)$, $b(t_i)$, and $b(t_f)$.

Using Eq. 1 *c*, the value of the first derivative of scattered light intensity with respect to cell volume, $a(V,t_i)$, at initial time, t_i, and at an arbitrary cell volume, V, may be expressed in terms of this derivative at initial time and isotonic cell volume, $a(V_{iso}, t_i)$, and the second derivative of intensity with respect to volume, $b(t_i)$:

$$a(V,t_i) \approx a(V_{iso},t_i) + b(t_i)(V - V_{iso}). \quad (1\,c')$$

The value of the first derivative of intensity with respect to volume at final time, t_f, and arbitrary volume may be similarly written:

$$a(V,t_f) \approx a(V_{iso},t_f) + b(t_f)(V - V_{iso}). \quad (1\,c'')$$

Subtracting Eq. 1 *c'* from Eq. 1 *c''*, we obtain

$$a(V,t_f) \approx a(V,t_i) + \alpha + \beta\,(V - V_{iso}), \quad (17)$$

where α is the difference in the first derivative at isotonic cell volume between final and initial times,

$$\alpha = a(V_{iso},t_f) - a(V_{iso},t_i), \quad (17\,a)$$

and β is the difference in the second derivative between final and initial times,

$$\beta = b(t_f) - b(t_i). \quad (17\,b)$$

The quantities we need to determine now are the first and second derivatives of intensity with respect to cell volume at initial time and isotonic cell volume, $a(V_{iso},t_i)$ and $b(t_i)$, and the differences between these derivatives at final and initial times, α and β.

For each set of experiments, the quantities α and β in Eq. 17 were calculated using the change, during each experiment, in the difference function calculated using controls at the initial volume *minus* the change in the difference function using the controls at the final volume (see legend to Fig. 6). Using Eqs. 1′ and 1 *c*, this "double difference" can be shown to be approximately equal to the difference between the first derivative of intensity with respect to volume at final time and the same derivative at initial time, both at the average cell volume during the experiment, $\bar{V}$,

$$a(\bar{V},t_f) - a(\bar{V},t_i) \approx \{[I_{DIF}(V_f,V_i^0,t_f) - I_{DIF}(V_i,V_i^0,t_i)] - [I_{DIF}(V_f,V_f^0,t_f) - I_{DIF}(V_i,V_f^0,t_i)]\}/(V_f - V_i) \quad (17\,c)$$

$$\approx \alpha + \beta(\bar{V} - V_{iso}). \quad (17')$$

Each combination of one experimental curve and two control curves yielded one data point in the linear regression for α and β.

The derivatives $a(V_{iso},t_i)$ and $b(t_i)$ were determined in two ways, and the results were averaged. The first method employed Eq. 1 with $t = t_i$ and $V_0 = V_{iso}$:

$$I(V,t_i) \approx I(V_{iso},t_i) + a(V_{iso},t_i)(V - V_{iso}) + b(t_i)(V - V_{iso})^2/2 \quad (1'')$$

For each set of experiments, using cells from one subject, the three parameters $I(V_{iso},t_i)$, $a(V_{iso},t_i)$, and $b(t_i)$ were determined by a least squares fit of Eq. 1″ to the intensities of light (extrapolated to zero time) scattered by cells at each of the volumes studied. The intensities of light scattered by cells of constant volume and by cells of

changing volume were both included. For the experimental runs (with cells of changing volume), the extrapolation of scattered light intensity to zero time, $I^{EXP}(V_i,t_i)$, was carried out by linear regression using the first 0.2 s of data in these experiments. For the control runs, the value of scattered light intensity at zero time, $I^{CTL}(V_0,t_i)$, was calculated from the scattered intensity at zero time in the experimental runs, $I^{EXP}(V_i,t_i)$, and the value of the difference, $I_{DIF}(V_i,V_0,t_i)$, between the experimental and the control runs at zero time, as determined by the χ^2 minimization routine (Eqs. 8–11),

$$I^{CTL}(V_0,t_i) \approx I^{EXP}(V_i,t_i) - I^{DIF}(V_i,V_0,t_i). \quad (2')$$

For each value of the experimental intensity extrapolated to zero time, two values of the control intensity at zero time were obtained, one for control runs using cells of volume, V_0, equal to that of the cells in the experimental runs at zero time, V_i, the other using cells of volume, V_0, equal to that of the cells in the experimental runs at the final time during the experiment, V_f.

The second method of calculating $a(V_{iso},t_i)$ and $b(t_i)$ used the difference between the initial and final values of the difference function for each combination of experimental and control runs. Using Eqs. 1′ and 1 *c*, we find that

$$[I_{DIF}(V_f,V_f^0,t_f) - I_{DIF}(V_i,V_f^0,t_i)]/(V_f - V_i) \approx a(V_{iso},t_i) + b(t_i)(\bar{V} - V_{iso}). \quad (18)$$

Similarly,

$$\frac{[I_{DIF}(V_f,V_i^0,t_f) - I_{DIF}(V_i,V_i^0,t_i)]}{(V_f - V_i)} - [a(\bar{V},t_f) - a(\bar{V},t_i)] \approx a(V_{iso},t_i) + b(t_i)(\bar{V} - V_{iso}), \quad (19)$$

where the quantity $a(\bar{V},t_f) - a(\bar{V},t_i) = \alpha + \beta(\bar{V} - V_{iso})$ has already been calculated (Eq. 17′). Using the values of the difference function at initial and final times for each pair of experimental and control runs in a set of experiments, the values of $a(V_{iso},t_i)$ and $b(t_i)$ in Eq. 18 and 19 were calculated by linear regression. Since the same data were used in Eqs. 1″, 17 *c*, 18, and 19, the four regressions do not give completely independent values of the derivatives, $a(V_{iso},t_i)$, $a(V_{iso},t_f)$, $b(t_i)$, and $b(t_f)$. Consequently, the variances in these quantities, determined as though each estimate of their values was independent, may be somewhat underestimated.

Calculation of the Constants F_1, F_2, and F_3

To estimate the values of these constants and the uncertainties associated with them, the functions $S(t)$ and $T(t)$ in Eqs. 9 and 14 were calculated at 0.1-s intervals from 0.1 to 3.0 s for one combination of experimental and control curves for each subject. The value of each of the constants was then calculated for all combinations of $S(t)$ from one experiment and $T(t)$ from the same or a different experiment. The average value and variance of each "constant" were estimated from these data.

Major Sources of Error

The primary instrumental source of error in the stop-flow determination of L_p arises from neglecting the nonlinearities in the relationship between changes in scattered light intensity and changes in cell volume. Even after correction of these errors by Eqs. 15 and 16, substantial uncertainty remained in our results, because the values of the coefficients F_1, F_2, and F_3 were assumed to be constant for all experiments. Although the values of F_2 and F_3 were not well determined (see Table II), they had

little effect on the results of these experiments. When F_2 and F_3 were set equal to zero, the value of the ratio of $L_{p,in}$ to $L_{p,out}$ obtained was 0.95 + 0.05, as before (Table III). The value of $\Delta L_p/\Delta$ (π_{iso}/π) obtained was 0.2 ± 0.4, only slightly more positive than before (Table III).

In Eq. 1 the intensity of scattered light was assumed to be a single-valued function of time and cell volume. This assumption is supported by Fig. 3, which shows that the light scattered by cells 2 s after mixing is essentially independent of whether the cells had swelled, shrunk, or remained at constant volume. The scattered light intensity in any set of identical single experimental runs varied by an amount roughly corresponding to a 1% cell volume change. The effect of this apparently random baseline variation was reduced by averaging the values obtained in a number of identical experiments.

The effect of the variation of the index of refraction on the intensity of scattered light was small. For a single experiment, it corresponded to a <0.002% cell volume change, and over a set of experiments the effect corresponded to a <1.6% cell volume change.

The uncertainty of about 1.5% in the osmolalities of our solutions was due (*a*) to an uncertainty of <1% in the osmolality determination; (*b*) to changes of <0.3% due to changing cell volume during an experiment; and (*c*) to a <1% uncertainty in the relative rates of delivery of the two syringes. The errors in apparent nonosmotic volumes arose partly from the errors in the determination of the osmolality of the solutions and partly from neglect of the correction for trapped extracellular fluid in our hematocrit measurements, which caused an error of <1%.

The error in elapsed time depended on the sampling time interval, the effect of the unstirred layer, the uncertainty in dead time, and the time required for intracellular mixing. The unstirred layer effect was the largest of these. Sha'afi et al. (1967) have shown that in their apparatus the effect of the unstirred layer was to delay contact between the cells and the newly mixed solutions by ~10 ms. Their observation tube was identical to ours, and the velocity of fluid in their observation tube was in the same range of 375–600 cm s^{-1}, so we have assumed an error in time of ~10 ms due to this effect. Our sampling time interval of 4.5–5 ms introduced an uncertainty of ~2.5 ms, and our uncertainties in dead time were ~2 ms. Finally, Paganelli and Solomon (1957) have shown that intracellular mixing is about 90% complete in 0.2 ms. These errors lead to a total time uncertainty of ~10 ms.

The light source heated the solutions by an average of 1°C as they passed through the apparatus. The solution in the observation tube may have been heated somewhat more than the average, but we estimate that if 10% of the total light energy incident upon the observation tube was absorbed by the fluid in it, this local heating would be <2°C s^{-1}. We have neglected this potential additional heating and have used the variation in the temperatures as an estimate of our error.

Evans and Fung (1972) have found that the red cell surface area varies by ~7% over the range of external osmolalities of 135–300 mosM. Since our range of osmolalities was 185–365 mosM, we have used 5% as the cell surface error estimate. Since the red cell membrane is essentially impermeable to cations over the 2-h time period of these experiments, solute permeation through the membrane is probably not much greater than that due to the chloride shift described by Gary-Bobo and Solomon (1968), which has an effect of <4% on our calculated values of L_p.

In Eq. 6, it is assumed that the cellular and extracellular solutions are sufficiently close to equilibrium that the phenomenological forces and flows across the membrane are linearly related (Kedem and Katchalsky, 1958). We have attempted to minimize the red cell volume changes used in these experiments to satisfy this condition but do

not have enough data to determine whether the value of L_p extrapolated to zero flow is different from that which we have calculated. It has been assumed that a pseudo-steady state is established across the red cell membrane during an experiment. This is probably the case, since the exchange time for diffusion of water across the red cell membrane is ~0.02 s (Paganelli and Solomon, 1957) more than an order of magnitude shorter than the half time for internal osmolality changes in our experiments.

The weighting factors σ_j^2 in Eqs. 10–15 were calculated by adding the variances in the calculated values of L_p at time t_j due to uncertainties in the values of the experimental and control intensities, nonosmotic volume, osmolalities, time, and temperature. Uncertainties in the scattered light intensity were the most significant.[5] The error estimate for the average value of L_p for a given difference function was obtained by adding each of the systematic variances in the mean value of L_p to the variance in the mean value of L_p due to random errors. The variance in the average value of L_p determined, using one experimental set of data and two control sets, was taken to be the average value of the variance estimated for the two combinations of experimental and control curves.

These estimates of error do not take into account the uncertainty due to differences in the properties of red cells of different subjects. This biological variation causes a further increase in the uncertainty in L_p beyond that discussed explicitly in this appendix (see text). These biological variations have been included in the final values for L_p.

We would like to thank Messrs. R. E. Dooley and W. Kazolias who constructed the mechanical parts of the equipment, Dr. A. Pandiscio who designed many of the electrical circuits, and Mr. Bernard Corrow who constructed them. We would also like to thank Dr. Bernard Chasan for his help in carrying out some of the experiments and Mr. Alan Verkman for suggesting the three-parameter fitting routine.

This research was supported in part by Energy Research and Development Administration Contract EY-76-S-02-3010. T. C. Terwilliger has been the holder of a National Science Foundation Graduate Fellowship.

Received for publication 18 January 1980.

REFERENCES

BLUM, R. M., and R. E. FORSTER. 1970. The water permeability of erythrocytes. *Biochim. Biophys. Acta.* **203:**410–423.

COLOMBE, B. W., and R. I. MACEY. 1974. Effects of calcium on potassium and water transport in human erythrocyte ghosts. *Biochim. Biophys. Acta* **363:**226–239.

EVANS, E., and Y. C. FUNG. 1972. Improved measurements of the erythrocyte geometry. *Microvasc. Res.* **4:**335–347.

FARMER, R. E. L., and R. I. MACEY. 1970. Perturbation of red cell volume: rectification of osmotic flow. *Biochim. Biophys. Acta.* **196:**53–65.

GALEY, W. R. 1978. Determination of human erythrocyte membrane hydraulic conductivity. *J. Membr. Sci.* **4:**41–49.

GARY-BOBO, C. M., and A. K. SOLOMON. 1968. Properties of hemoglobin solutions in red cells.

[5] The uncertainties due to the variances in the coefficients in Eqs. 15 and 16 were not included. Although this variance was the major source of uncertainty in the average overall value of L_p for an experiment, for a calculation of L_p at a particular time the variances due to the uncertainty in the intensity of scattered light were far greater.

J. Gen. Physiol. **52**:825–853.

JAY, A. W. L. 1975. Geometry of the human erythrocyte. *Biophys. J.* **15**:205–222.

KEDEM, O., and A. KATCHALSKY. 1958. Thermodynamic analysis of the permeability of the biological membranes to non-electrolytes. *Biochim. Biophys. Acta.* **27**:229–246.

LEVIN, S. W., R. L. LEVIN, and A. K. SOLOMON. 1980. Improved stop-flow apparatus to measure permeability of human red cells and ghosts. *J. Biochem. Biophys. Methods.* **3**:255–272.

PAGANELLI, C. V., and A. K. SOLOMON. 1957. The rate of exchange of tritiated water across the human red cell membrane. *J. Gen. Physiol.* **41**:259–277.

PAPANEK, T. H. 1978. The water permeability of the human erythrocyte in the temperature range +25°C to −10°C. Ph.D. Thesis. Massachusetts Institute of Technology, Cambridge, Mass.

RICH, G. T., R. I. SHA'AFI, A. ROMUALDEZ, and A. K. SOLOMON. 1968. Effect of osmolality on the hydraulic permeability coefficient of red cells. *J. Gen. Physiol.* **52**:941–954.

SAVITZ, D., V. W. SIDEL, and A. K. SOLOMON. 1964. Osmotic properties of human red cells. *J. Gen. Physiol.* **48**:79–94.

SHA'AFI, R. I., G. T. RICH, V. W. SIDEL, W. BOSSERT, and A. K. SOLOMON. 1967. The effect of the unstirred layer on human red cell water permeability. *J. Gen. Physiol.* **50**:1377–1399.

SIDEL, V. W., and A. K. SOLOMON. 1957. Entrance of water into human red cells under an osmotic pressure gradient. *J. Gen. Physiol.* **41**:243–257.